

# Catalytic combustion of methane over hexaaluminates $Ba_{1-x}La_xAl_{11}O_{19\pm\delta}$ supported on mullite honeycomb

Xiangbo Feng<sup>1</sup>, Zhiguo Qu<sup>\*2</sup>

<sup>1</sup>School of Energy and Power Engineering, Xi'an Jiaotong University, Xi'an, China

<sup>2</sup>School of Energy and Power Engineering, Xi'an Jiaotong University, Xi'an, China

## Abstract

The study investigated the methane combustion in a  $Ba_{1-x}La_xAl_{11}O_{19\pm\delta}$  supported on mullite honeycomb burner. Effects of La substitution ratio (x) and air preheated temperature ( $T_p$ ) on the catalytic combustion performances were evaluated. The flame stability limits expanded with increased  $T_p$  or x. The surface temperature uniformities enhanced and the flame front location moved the upstream zone with increased  $T_p$  or x. The flue gas temperatures lowered with increased x. The flue gas temperatures decreased firstly, and continually increased with improved  $T_p$ . Both the HC and CO emissions decreased significantly with increased  $T_p$  or x. The NO<sub>x</sub> emissions decreased with increased x. The NO<sub>x</sub> emission decreased firstly, and then increased with improved  $T_p$ . The variation trends were nearly consistent with the flue gas temperatures.

## Introduction

In recent decades, catalytic combustion of natural gas has been widely investigated as an alternative to conventional combustion due to its superior practical applications for pollution abatement and power generation. By enabling the use of very lean mixtures and reducing combustion temperatures, catalytic combustion offers the possibility of producing heat and energy at much lower temperatures, thus significantly reducing the emissions of pollutants such as CO, NO<sub>x</sub> and unburned hydrocarbons (HC) [1-4].

Nevertheless, a lack of catalyst materials having sufficient high-temperature stability and durability is a principal problem for developing high-temperature catalytic combustion applications. Catalyst material development is therefore one of key issues in elevated temperature catalytic combustion [5]. Hexaaluminate materials are one of the desired catalysts [6, 7]. Hexaaluminates can be represented by the general formula  $AB_xAl_{12-x}O_{19}$ , where A represents an alkaline, alkaline-earth or rare-earth metal ion, and B a transition-metal ion with similar size and charge as aluminum. Substituting a few of the aluminum ions with transition-metals ions can substantially increase the oxidation activity of the material while retaining a similar sintering resistance compared to the non-substituted material [8]. For high-temperature combustion, the ideal catalyst material should have low-temperature activity and high-temperature stability. Substituted hexaaluminates  $Ba_{1-x}La_xMnAl_{11}O_{19-\alpha}$  can offer great promise to meet the aforementioned demands [9, 10]. Hexaaluminates are less active than traditional palladium and platinum catalysts, whereas thermal stability and resistance were extremely superior to the latter.

Amounts of studies reported the superior thermal stability of La/Ba/Mn/Sr hexaaluminates compared with other catalysts [11, 12]. Sidwell et al. [7] studied the behavior of methane/air combustion on a  $La_{0.267}Sr_{0.333}Mn_{0.4}Al_{11}O_{18}$  hexaaluminate catalyst in a stagnation flow. Results indicate that the catalyst surface is affecting the gas-phase chemistry and the hexaaluminate catalyst surface acts as a sink for methyl radicals, which suppress the gas-phase reaction. In addition, the hexaaluminate catalyst exhibits good high-temperature activity and retains its activity after exposure to temperatures of 1110°C. Li and Wang [13] prepared the Mn-substituted Ba-La-hexaaluminate catalysts with surface area in the range between 45 and 73 m<sup>2</sup>/g, and indicates the  $Ba_{0.2}La_{0.8}MnAl_{11}O_{19-\alpha}$  possesses the highest catalytic activity owing to the excellent performance of activating oxygen. Kim et al. [14] investigated Mn-substituted La, Sr-hexaaluminate catalysts for the catalytic combustion of offgas. The catalytic activity and thermal stability were tested under simulated PSA offgas condition, results indicate that the  $La_{0.6}Sr_{0.4}MnAl_{11}O_{19}$  owns the most active and retains its lattice structure and chemical composition at 1000°C about 40h.

Recently, extensive studies on further improving the combustion performances, such as expanding flame stability limits and lowering pollution emissions, have been investigated. One of the most important solutions is optimizing the operating conditions. Zhao et al. [15] investigated the effect of air preheating and moisture level on combustion characteristics. The results indicate that the total burning time is shorter and produces lower ignition front flame temperature under the higher primary air preheating temperature. Huang et al. [16] examined the effect of air preheat temperature on moderate or intense low-oxygen dilution combustion of coal-derived syngas, and

\*Corresponding author: [zgqu@mail.xjtu.edu.cn](mailto:zgqu@mail.xjtu.edu.cn)

concludes that the lean operational limit expands and the NO<sub>x</sub> and CO emissions suppress under air preheating conditions. Zhang et al. [17] developed a high temperature air combustion technology for energy saving, flame stability enhancement, and NO<sub>x</sub> emission reduction. Results reveal that practicability of the HTAC technology using the proposed approach is confirmed for efficiently and cleanly burning fuels. Kessel et al. [18] experimentally investigated solid fuel grate combustion in a pot furnace both with and without primary air preheating conditions. Results conclude the preheating of the primary air acts as a catalyst for the ignition. Based on the above reviews, air preheating [19, 20] is a significant impact on flame stability, flame temperature, combustion efficiency, and pollutant emissions. However, most of studies mainly focus on the inert combustion, the effect of air preheating temperature on catalytic combustion performances have been little reported.

In this study, the catalytic performances of substituted Ba-La hexaaluminates Ba<sub>1-x</sub>La<sub>x</sub>Al<sub>11</sub>O<sub>19±δ</sub> supported on 200 cpsi mullite honeycomb substrates were prepared and used in lean methane-air combustion. The catalytic combustion performances of flame stability limits, surface temperature distributions of honeycombs catalysts, flue gas temperatures, and pollutant emissions were evaluated. The experimental study mainly investigated the effects of air preheating temperature (Tp) and La substitution ratio (x) on the catalytic combustion performances.

## Materials and methods

### Preparation of catalysts

The substituted Ba-La hexaaluminates Ba<sub>1-x</sub>La<sub>x</sub>Al<sub>11</sub>O<sub>19±δ</sub> samples were prepared by co-precipitation procedures, which were derived from the published study by Kim et al. [14]. Stoichiometric amounts of La(NO<sub>3</sub>)<sub>3</sub>·8H<sub>2</sub>O, Ba(NO<sub>3</sub>)<sub>2</sub>·4H<sub>2</sub>O, and Al(NO<sub>3</sub>)<sub>3</sub>·9H<sub>2</sub>O were dissolved in deionized water, separately. Precursor solutions of Ba and La were poured into the aluminum nitrate solution at 80 °C. Ammonium carbonate solution was added until the pH of the solution reached 7–9. The solution was aged for 5 h at 80 °C under vigorous stirring, and then the precipitate was filtered and washed with deionized water. After 12h at room temperature, then the precipitates were evaporated under reduced pressure. The powders obtained were dried for 3h at 120 °C in oven, followed by calcination in a quartz call at 1200 °C for 24h under a flow of oxygen. This temperature was necessary to ensure the complete formation of the hexaaluminate phase. The catalysts issued from this calcination will be referred to as fresh catalysts.

The 200cpsu mullite honeycombs (3Al<sub>2</sub>O<sub>3</sub>·SiO<sub>2</sub>) required pretreatments before the catalysts powders were deposited on the honeycombs supports. The pretreated supports were impregnated in the slurry of hexaaluminates. The coated honeycombs catalysts were then dried and weighed. The impregnating

processes were repeated several times to ensure that the Ba<sub>1-x</sub>La<sub>x</sub>Al<sub>11</sub>O<sub>19±δ</sub> content was 5.0 wt. %. After the honeycombs catalysts were reduced with hydrazine, filtered, and washed with large amounts of deionized water, the honeycombs catalysts were dried in an oven at 200 °C for 12 h. The honeycombs catalysts were then calcined for 4 h in a vacuum furnace at a temperature of 1200 °C to maintain thermal stability. Then, final 200cpsu mullite honeycombs supported substituted Ba-La hexaaluminates catalysts (5.0 wt. % Ba<sub>1-x</sub>La<sub>x</sub>Al<sub>11</sub>O<sub>19±δ</sub>/3Al<sub>2</sub>O<sub>3</sub>·SiO<sub>2</sub>) were obtained.

### Catalysts characterization

The specific surface areas (SSA) of hexaaluminates catalysts Ba<sub>1-x</sub>La<sub>x</sub>Al<sub>11</sub>O<sub>19±δ</sub>/3Al<sub>2</sub>O<sub>3</sub>·SiO<sub>2</sub> with different La substitution ratios x both in fresh and in methane combustion conditions were obtained using an automatic gas sorption analyzer apparatus based on N<sub>2</sub> adsorption isotherms and the Brunauer–Emmett–Teller (BET) method. Table 1 presents the BET testing results. The results indicated that the specific surface areas of the hexaaluminates catalysts dramatically increased with increased x. All the specific surface areas of the hexaaluminates catalysts decreased to a particular extent after combustion, whereas the reduction ranges decrease with increased x.

Table 1. SSA of Ba<sub>1-x</sub>La<sub>x</sub>Al<sub>11</sub>O<sub>19±δ</sub>/3Al<sub>2</sub>O<sub>3</sub>·SiO<sub>2</sub>

Catalyst sample	BET surface area (m <sup>2</sup> g <sup>-1</sup> )			
	Fresh	600 °C	1000 °C	1200 °C
Ba <sub>1-x</sub> La <sub>x</sub> Al <sub>11</sub> O <sub>19</sub> /3Al <sub>2</sub> O <sub>3</sub> ·SiO <sub>2</sub>				
x=0	63.10	48.90	20.50	6.90
x=0.20	91.50	63.50	39.20	19.70
x=0.40	110.50	74.90	47.10	24.90
x=0.60	115.90	82.50	58.30	33.50
x=0.80	118.50	89.50	65.30	45.30

### Experimental setup

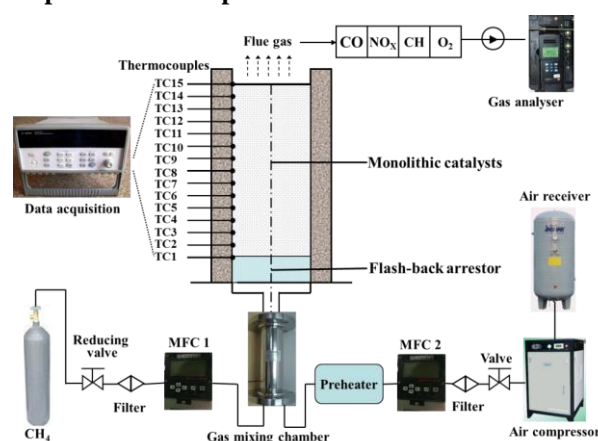


Fig. 1. Schematic of catalytic combustion system

The schematic of catalytic combustion system is shown in Fig. 1. Methane is supplied by a high pressurized bottle with a purity of 99.9%, was used as the fuel, reducing value and filter are used before being introduced into mass flow controller 1 (MFC 1) to reduce the pressure to 0.4Mpa and further remove the impurities, respectively. Laboratory air is supplied by

an air compressor via an air reduce receiver to lower the pressure, and air filter is used before being introduced into the mass flow controller 2 (MFC 2) to fully remove the moisture and impurities. The mass flow rate of methane and air are both controlled with MFC 1 and MFC 2, respectively. The adjusted fuel and air via two MFCs are uniformly mixed in gas mixing chamber. The mixing chamber is designed to ensure the fuel and air were uniformly premixed and to maintain a constant equivalence ratio of the mixture. Then, the mixed gas enters into the burner. In the burner entrance, a flash-back arrestor is applied to prevent flash-back. The burner is a corundum with diameter of 50 mm, thickness of 10 mm, and height of 175 mm. Three 200 cpsi honeycombs supported  $Ba_{1-x}La_xAl_{11}O_{19\pm\delta}/3Al_2O_3\cdot SiO_2$  hexaaluminates catalysts sections were arranged on the flash-back arrestor. Fifteen K-type thermocouples (TC1-TC15) were located at 10 mm intervals along the axial length direction to monitor surface temperature distribution of hexaaluminates catalysts. All signals of thermocouples are recorded using a data acquisition system. The flue gas was extracted and collected using a stainless steel probe placed at the outlet of burner. The flue gas temperature ( $T_f$ ) and pollutants emissions of HC, CO, and  $NO_x$  were measured by a flue gas analyzer.

## Results and discussion

### Flame stability limits versus $T_p$ and $x$

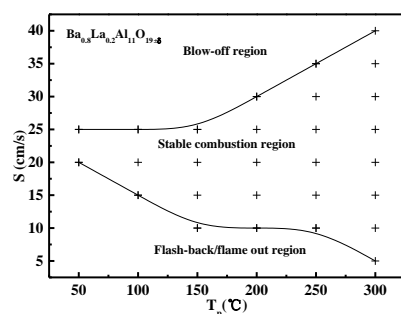


Fig. 2 Effect of  $T_p$  on the flame stability limits

The flame stability limits is defined as the maximum and the minimum mixed gas inlet velocity ( $S$ ) that the flame front can sustained in the honeycombs catalysts regions at given operating conditions. The lower flame stability limit is defined as the  $S$  at which the flame front moved the location of thermocouple TC1, below this smallest  $S$ , a flash-back or flameout happens. The upper flame stability limit is defined as the  $S$  at which the flame front floated on the burner exit (TC 15), and above which, blow off will occur. Fig.2 shows the flame stability limits of burner for  $Ba_{0.8}La_{0.2}Al_{11}O_{19\pm\delta}/3Al_2O_3\cdot SiO_2$  honeycomb catalyst versus air preheated temperature  $T_p$ . The lower flame stability limit gradually lowered with improved  $T_p$ , whereas the upper flame stability limit significantly increased with improved  $T_p$ , resulting in the flame stability limits significantly expanded with improved  $T_p$ . The above results were mainly caused by the two reasons. On one hand, the temperatures of inlet mixed

gas and the solid catalyst were significantly heated with the improved  $T_p$ . The activation energy of methane reduced and the catalytic activity of monolithic catalyst enhanced, which reduced the combustion temperature and fuel values required for stable combustion. The reduction of methane activation energy and the enhancement of catalyst activity jointly decreased the lower flame stability limit. On the other hand, the heterogeneous catalytic combustion were strengthened with the improved  $T_p$  and the residence time of mixed gas within the burner had been shortened, resulting in the impact of increasing the  $S$  on the flame front location had been weakened and the speed of the flame front moved to the burner exit reduced, the two facts induced that the maximum  $S$  increased at given flame front location with improved  $T_p$ , which increased the upper flame stability limit.

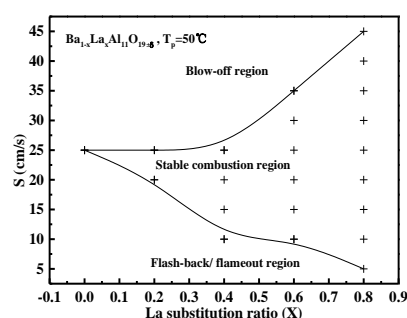


Fig. 3. Effect of  $x$  on the flame stability limits.

Fig. 3 shows the flame stability limits of burner for  $Ba_{0.8}La_{0.2}Al_{11}O_{19\pm\delta}/3Al_2O_3\cdot SiO_2$  honeycombs catalysts with different La substitution ratios  $x$ . With increase of  $x$ , the lower flame stability limit lowered and the upper flame stability limit improved, resulting in significant enlargement of flame stability limits with increased  $x$ . The specific surface areas of honeycombs catalysts both in fresh and in combustion conditions significantly enhanced with increased  $x$ , resulting in enhancing the catalytic activity and improving the gas mixing uniformity. The enhancement of catalytic activity improved the methane combustion rate and reduced the fuel and temperature value required for stable combustion, which lowered the lower flame stability limit. The effect of an increase in  $S$  on stable combustion had been weakened because the inhibition effects of gas phase combustion had been strengthened. The mixed gas diffusion was improved with increased  $x$  because of enhancement of specific surface area. The indicated inhibition effects of gas phase combustion and improved mixed gas diffusion corporately induced the increase in upper flame stability limit.

### Surface temperature distribution of honeycomb catalyst (TC) versus $T_p$ and $x$

Fig. 4 shows the surface temperature distribution of honeycomb catalyst versus air preheated temperature  $T_p$  with gas velocity of  $S=25\text{cm/s}$ . The flame front can be identified as the location where the TC reached the maximum value ( $TC_{\max}$ ) and the change trend of flame temperature was nearly consistent with the  $TC_{\max}$ . With improved  $T_p$ , the flame

front location gradually moved to upstream zone and the uniformities of TC had been enhanced, whereas, the  $TC_{max}$  decreased firstly, and then increased with continually improved  $T_p$ . The reason was that both the mixed gas preheating performance and the catalyst activity enhanced with improved  $T_p$ . The indicated facts promoted the enhancement of the catalytic combustion performance and the time for burning the methane had been shortened, resulting in the flame front location moved to the upstream zone. Heat transfer and diffusion performance between the mixed gas and catalyst surface enhanced with improved  $T_p$ , in which the diffusion uniformity of mixed gas throughout honeycomb catalyst improved and the local flame temperature reduced. Therefore, the  $TC_{max}$  decreased because of reduction of local flame temperature. Comparatively, the  $TC_{max}$  began to increase as the  $T_p$  continuously increased to 300°C. The result was attributed that the local flame temperature gradually improved because the gas phase's temperature increased.

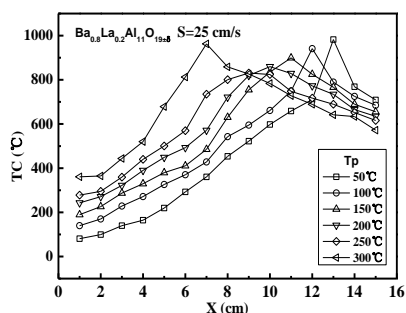


Fig.4 Effect of  $T_p$  on TC( $S=25\text{cm/s}$ )

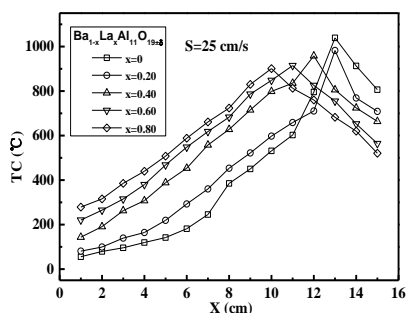


Fig. 5 Effect of  $x$  on TC ( $S=25\text{cm/s}$ ).

The surface temperature distributions of honeycombs catalysts  $Ba_{1-x}La_xAl_{11}O_{19\pm\delta}/3Al_2O_3.SiO_2$  versus La substitution ratio  $x$  is illustrated in Fig. 5. With increased  $x$ , the TC near the burner entrance region increased and near the burner exit region decreased, the distribution uniformity of TC enhanced, and the  $TC_{max}$  decreased. These facts were due to the improved heat mass transfer performance and enhanced catalytic activity caused by increased specific surface area that resulted the enhanced preheating effect near the burner entrance. In addition, the extended specific surface area for increased  $x$  significantly enhanced the heat recirculation and feedback from near the flame front region to near the burner entrance region because of the improved gas

mixing and diffusion performance. The indicated causes induced the enhancement of TC distribution uniformity and the decrease of  $TC_{max}$ .

### Flue gas temperature ( $T_f$ ) of catalytic burner versus $T_p$ and $x$

Fig. 6 presents the flue gas temperature of  $Ba_{0.8}La_{0.2}Al_{11}O_{19\pm\delta}/3Al_2O_3.SiO_2$  versus gas velocity  $S$  with different air preheated temperatures  $T_p$ . The variation trends of  $T_f$  with increased  $T_p$  were generally analogical to the relationship between the  $TC_{max}$  and the increase of  $T_p$ . The  $T_f$  decreased as the  $T_p$  increased ranging from 50°C to 250°C, but increased as the  $T_p$  continuously increased from 250°C to 300°C. With the improved  $T_p$ , methane activation energy reduced and catalytic combustion rate increased, resulting in decreasing the flue gas temperature because the residence time of gas phases within burner had been shortened. In addition, enhanced gas-solid catalytic combustion significantly restricted the gas-phase combustion, which contributed to the decrease of gas-phase combustion rate, ultimately resulting in reducing the flue gas temperature.

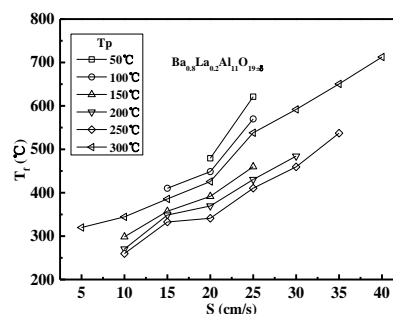


Fig. 6 Effect of  $T_p$  on  $T_f$ .

Fig. 7 shows the flue gas temperature versus gas velocity  $S$  for  $Ba_{1-x}La_xAl_{11}O_{19\pm\delta}/3Al_2O_3.SiO_2$  with different La substitution ratios  $x$ . The results indicated that the  $T_f$  decreased with increased  $x$ . The  $TC_{max}$  decreased with increase of  $x$  as indicated in Fig. 5, which tended to decrease the flue gas temperature. In addition, the specific surface area increased and the catalytic activity enhanced with increased  $x$ , resulting in decreasing the flue gas temperature because enhanced catalytic combustion extremely inhibited the gas phase combustion.

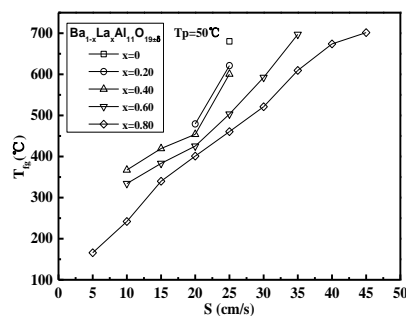


Fig. 7 Effect of  $x$  on  $T_f$ .

### HC emission of catalytic burner versus $T_p$ and $x$

Fig. 8 presents the HC emission of catalytic burner

versus gas velocity  $S$  for  $Ba_{0.8}La_{0.2}Al_{11}O_{19\pm\delta}/3Al_2O_3 \cdot SiO_2$  with different air preheated temperatures  $T_p$ . HC emission was mainly controlled by gas-solid heterogeneous catalytic combustion, specific surface area of catalyst, heat feedback, gas mixing performance, and diffusion rate of mixed gas. The HC emission significantly decreased with the improved  $T_p$ . The temperature of both gas phases and solid catalyst improved with the improved  $T_p$ , resulting in more complete methane combustion and reducing the HC emission because the heat input increased and the methane activation energy reduced.

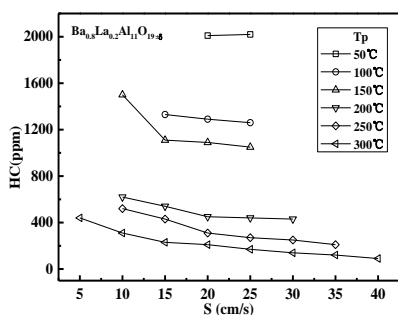


Fig. 8 Effect of  $T_p$  on HC emissions.

The HC emissions of catalytic burner versus gas velocity  $S$  for  $Ba_{1-x}La_xAl_{11}O_{19\pm\delta}$  catalysts with different La substitution ratios  $x$  is illustrated in Fig. 9. The HC emissions dramatically decreased with increased  $x$ . The specific surface area of catalyst both in fresh and  $r$  combustion conditions significantly improved with increased  $x$ , which the gas mixing performance and the diffusion rate of mixed gas also enhanced. The improved gas mixing performance and the diffusion rate of mixed gas within the burner intensified the gas-solid catalyst heterogeneous catalytic combustion performance, resulting in decreasing the HC emission.

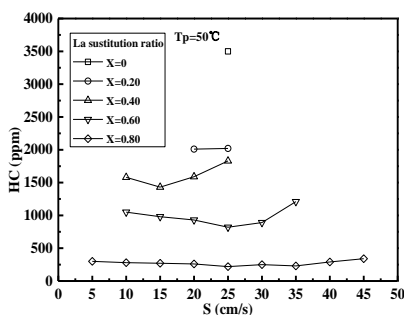


Fig. 9 Effect of  $x$  on HC emissions.

#### CO emission of catalytic burner versus $T_p$ and $x$

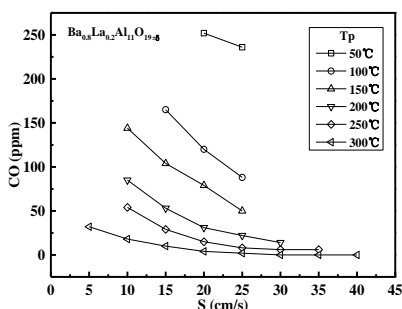


Fig. 10 Effect of  $T_p$  on CO emissions

Fig. 10 presents the CO emissions versus gas velocity  $S$  for  $Ba_{0.8}La_{0.2}Al_{11}O_{19\pm\delta}$  catalyst with different air preheated temperatures  $T_p$ . The CO emission was mainly affected by catalytic combustion effect, heat input, specific surface area of catalyst, and diffusion rate of mixed gas. The CO emission significantly decreased with increased  $T_p$  or  $S$ . The improved  $T_p$  tended to increase the heat input and improve the catalytic activity, resulting in decreasing the CO emission because the heat input of the burner improved and the catalytic combustion rate increased.

Fig. 11 presents the CO emission of catalytic burner versus gas velocity  $S$  for  $Ba_{1-x}La_xAl_{11}O_{19\pm\delta}$  catalysts with different La substitution ratios  $x$ . The CO emission dramatically decreased with increased  $x$ . With increased  $x$ , the specific surface area of catalyst increased and the mixed gas diffusion performance improved, resulting in significantly decrease in CO emission because of reinforced catalytic combustion and improved diffusion rate of mixed gas.

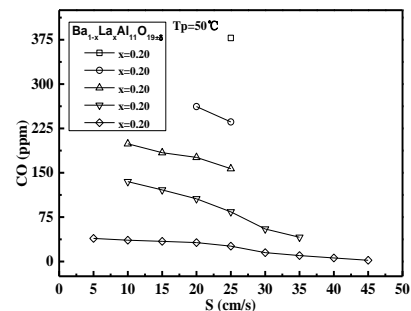


Fig. 11 Effect of  $x$  on CO emissions.

#### NOx emission of catalytic burner versus $T_p$ and $x$

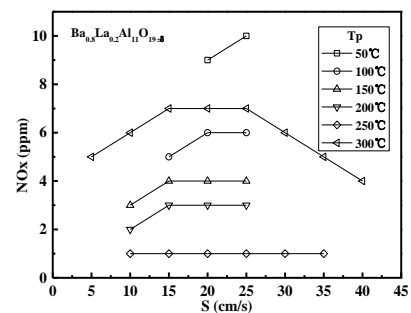


Fig. 12 Effect of  $T_p$  on NOx emissions

Fig. 12 shows the NOx emission of catalytic burner versus gas velocity  $S$  for  $Ba_{0.8}La_{0.2}Al_{11}O_{19\pm\delta}$  catalyst with different air preheating temperatures  $T_p$ . The NOx emissions reduced from 10 ppm to 1 ppm as the  $T_p$  increased from 50 °C to 250 °C, but continually improved the  $T_p$  to 300 °C, the NOx emissions began to increase to 7 ppm. As indicated in Fig. 4 and Fig. 6, both the  $TC_{max}$  and  $T_f$  decreased when the  $T_p$  increased from 50 °C to 250 °C, but increased as the  $T_p$  increased to 300 °C. The results illustrated that the NOx emission was mainly depended on the  $TC_{max}$  and  $T_f$ . The NOx emissions decreased as the  $T_p$  appropriately increased because the gas-solid heterogeneous catalytic

combustion improved and the gas phase combustion weakened. However, the NO<sub>x</sub> emission raised again as the  $T_p$  continuously increased to 300 °C because the gas phase temperature dramatically improved.

Fig. 13 presents the NO<sub>x</sub> emission of catalytic burner versus gas velocity  $S$  for Ba<sub>1-x</sub>La<sub>x</sub>Al<sub>11</sub>O<sub>19±δ</sub> catalysts with different La substitution ratios  $x$ . The NO<sub>x</sub> emissions reduced with increased  $x$  because the  $TC_{max}$  and  $T_f$  decreased. In addition, the gas phase temperature reduced with increased  $x$  because the reinforced gas-solid catalytic combustion restricted the gas-phase homogeneous combustion for the improved specific surface areas.

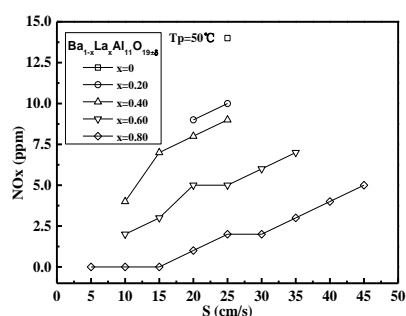


Fig. 13 Effect of  $x$  on NO<sub>x</sub> emissions.

## Conclusion

Ba<sub>1-x</sub>La<sub>x</sub>Al<sub>11</sub>O<sub>19±δ</sub> hexaaluminate supported on 200 cspi mullite honeycomb catalysts had been prepared and catalytic combustion performances for methane were studied. The effects of La substitution ratio ( $x$ ) and air preheated temperature ( $T_p$ ) on flame stability limits, surface temperature distributions of catalysts, flue gas temperatures, and pollutant emissions were evaluated. Results indicated that the  $x$  and  $T_p$  strongly influenced catalytic combustion properties. Specific surface areas and catalytic activities of catalysts dramatically enhanced with increased  $x$ . The flame stability limits expanded with increased  $T_p$  or  $x$ . The flame front gradually moved upstream region of catalysts with increased  $T_p$  or  $x$ . The TC had more uniform temperature contributions and  $TC_{max}$  decreased with increased  $T_p$  or  $x$ . The  $T_f$  decreased as the  $T_p$  increased from 50 °C to 250 °C, and decreased from 250 °C to 300 °C. The  $T_f$  also decreased with increased  $x$ . The HC emissions reduced with increased  $T_p$  or  $x$ . The CO emissions had the similar varied trends with the HC emissions. The NO<sub>x</sub> emissions reduced from 10 ppm to 1 ppm as the  $T_p$  increased from 50 °C to 250 °C, continually improving the  $T_p$  to 300 °C, the NO<sub>x</sub> emissions began to increase to 7 ppm. The NO<sub>x</sub> emissions dramatically reduced with increased  $x$ .

## Acknowledgment

This study was supported by the National Key Projects of Fundamental R/D of China (973 Project No. 2011CB610306) and the National Natural Science Foundation of China (No. 51322604).

## References

- [1] S. Su, X. X. Xu, *Energy*. 79(2015) 428-438.
- [2] P. S. Barbato, V. D. Sarli, G. Landi, A. D. Benedetto, *Chem. Eng. J.* 259 (2015) 381-390.
- [3] S. Karagiannidis, J. Mantzaras, K. Boulouchos, P. Combust. Inst. 33 (2011) 3241-3249.
- [4] J. Okal, M. Zawadzki, *Appl. Catal. A Gen.* 453 (2013) 349-357.
- [5] L. M. T. Simplicio, S. T. Brandao, D. Domingos, F. B.-Verduraz, E. A. Sales, *Appl. Catal. A Gen.* 360 (2009) 2-7.
- [6] E. E. Svensson, M. Boutonnet, S. G. Jaras, *Appl Catal. B Environ.* 84 (2008) 241-250.
- [7] R. W. Sidwell, H. Y. Zhu, R. J. Kee, D. T. Wickham, *Combust. Flame.* 134 (2003) 55-66.
- [8] G. Groppi, G. Cristiani, P. Forzatti, *J. Catal.* 13 (1997) 85-113.
- [9] T.V. Choudhary, S. Banerjee, V.R. Choudhary, *Appl. Catal. A Gen.* 234 (2002) 1-23.
- [10] K. Sekizawa, M. Machida, K. Eguchi, H. Arai, *J. Catal.* 142 (1993) 655-663.
- [11] G. Groppi, M. Belleto, C. Cristiani, P. Forzatti, P.L.Villa, *Appl. Catal. A Gen.* 104 (1993) 101-108.
- [12] B.W.-L Jang, R.M. Nelson, J.J. Spivey, M. Ocal, R.Oukaci, G. Marcelin, *Catal. Today.* 47 (1999) 103-113.
- [13] S. Q. Li, X. L. Wang, *J. Alloy. Compd.* 432 (2007) 333-337.
- [14] S. Kim, D.-W. Lee, J. Y. Lee, H.-J. Eom, H. J. Lee, I.-H. Cho, K.-Y. Lee, *J. Mol. Catal. A Chem.* 335 (2011) 60-64.
- [15] W. Zhao, Z. Q. Li, G. B. Zhao, F. S. Zhang, Q. Y. Zhu, *Energ. Convers. Manage.* 49 (2008) 3560-3565.
- [16] M. M. Huang, Z. D. Zhang, W. W. Shao, Y. Xiong, Y. Liu, F. L. Lei, *Energ. Convers. Manage.* 86 (2014) 356-364.
- [17] H. Zhang, G. X. Yue, J. F. Lu, Z. Jia, J. X. Mao, T. Fujimori, T. Suko, T. Kiga, *P. Combust. Inst.* 31 (2007) 2779-2785.
- [18] L. B. M. Kessel, A. R. J. Arendsen, P. D. M. Boer-meulman, G. Brem, *Fuel.* 83 (2004) 1123-1131.
- [19] Z.Q. Ouyang, J. G. Zhu, Q. G. Lu, *Fuel.* 113 (2013) 122-127.
- [20] Y. Huang, C. Y. H. Chao, P. Cheng, *Int. J. Heat. Mass. Tran.* 45 (2002) 4315-4324.